

Article

Development and Implementation of a Novel Optimization Algorithm for Reliable and Economic Grid-Independent Hybrid Power System

Mohammed Kharrich ¹, Omar Hazem Mohammed ², Salah Kamel ³, Ali Selim ^{3,4},
Hamdy M. Sultan ⁵, Mohammed Akherraz ¹ and Francisco Jurado ^{4,*}

¹ Department of Electrical Engineering, Mohammadia School of Engineers, Mohammed V University, Ibn Sina Street P.B 765, Rabat 10090, Morocco; mohammedkharrich@research.emi.ac.ma (M.K.); akherraz@emi.ac.ma (M.A.)

² Department of Technical Power Engineering, Technical College, Northern Technical University, Mosul 41002, Iraq; omar.hazem@ntu.edu.iq

³ Department of Electrical Engineering, Faculty of Engineering, Aswan University, Aswan 81542, Egypt; skamel@aswu.edu.eg (S.K.); ali.selim@aswu.edu.eg (A.S.)

⁴ Department of Electrical Engineering, University of Jaén, 23700 EPS Linares Jaén, Spain

⁵ Electrical Engineering Department, Faculty of Engineering, Minia University, Minia 61111, Egypt; hamdy.soltan@mu.edu.eg

* Correspondence: fjurado@ujaen.es

Received: 17 August 2020; Accepted: 16 September 2020; Published: 21 September 2020



Abstract: Recently, fast uptake of renewable energy sources (RES) in the world has introduced new difficulties and challenges; one of the most important challenges is providing economic energy with high efficiency and good quality. To reach this goal, many traditional and smart algorithms have been proposed and demonstrated their feasibility in obtaining the optimal solution. Therefore, this paper introduces an improved version of Bonobo Optimizer (BO) based on a quasi-oppositional method to solve the problem of designing a hybrid microgrid system including RES (photovoltaic (PV) panels, wind turbines (WT), and batteries) with diesel generators. A comparison between traditional BO, the Quasi-Oppositional BO (QOBO), and other optimization techniques called Harris Hawks Optimization (HHO), Artificial Electric Field Algorithm (AEFA) and Invasive Weed Optimization (IWO) is carried out to check the efficiency of the proposed QOBO. The QOBO is applied to a stand-alone hybrid microgrid system located in Aswan, Egypt. The results show the effectiveness of the QOBO algorithm to solve the optimal economic design problem for hybrid microgrid power systems.

Keywords: economic energy; Bonobo Optimizer; hybrid renewable energy system; microgrid; PV panels; wind turbine; energy storage

1. Introduction

Despite the steady increase in electric power production, it is still below the required level, due to the increase in load demand caused by the population increase as well as the increased use of technology in the residential, industrial and agricultural fields. According to the International Energy Agency (IEA), the global electricity demand will grow at an annual rate of 2.1% until 2040. This increases electricity's share in the total energy consumption to 24% in 2040. It is expected that renewable energy sources (RES) will face a significant increase in global investment in the coming years, to cover more than half of the energy consumption in the world by 2040. These energies will

make up for the shortfall in electrical energy production and contribute to a reduction in carbon dioxide emissions in the atmosphere, thereby reducing pollution significantly [1–3].

In order to invest in RES to optimize electrical energy production and raise the efficiency of the systems, many studies in the world recommend combining different technologies to form hybrid renewable energy systems (HRES) [4,5]. Consequently, these sources complement each other, support the national grid, and reduce the use of traditional power plants depending on fossil fuels that release greenhouse gases and pollute the environment [6]. However, the design of these hybrid systems needs sophisticated programs and smart algorithms capable of reaching the optimal solution taking into consideration all the conditions and constraints such as reliability aspects, economic cost, sensitivity factors, availability of RES, etc. [1,2,7,8].

Several studies have been conducted on the technical and economic feasibility of hybrid systems in past years to determine their viability. Many of these studies have used different modeling of HRES, and they have applied different algorithms and various software tools to achieve their goals. According to the literature, these challenges still exist and are the focus of a lot of research, especially on finding the best algorithms and modern techniques in reaching the optimal solutions of the optimization problem of finding the optimal sizing of the installed capacities of the components of HRES [9–15].

In [16], the pre-feasibility analysis of a stand-alone energy system using HRES including renewable and conventional energy sources was applied using HOMER software in Newfoundland, Canada. In one of the earlier studies [17], the authors conducted a feasibility study of generating electricity using RES for a hybrid system in a stand-alone village in Chhattisgarh, India. In [18], the authors introduce a realistic solution for energy demand from a hybrid power system consists of wind turbines (WT), photovoltaics (PV), and battery energy storage systems (BESS). Through a real measurement of meteorological data in 2017, concerning especially the wind speed, solar radiation and temperature, the output power of the proposed hybrid system is calculated. Load satisfaction is considered to evaluate the feasibility of the system. The optimum solution is found using the linear TORSCHÉ optimization technique, while a comparative study between PV/WT/battery and PV/WT has been accomplished and an economic analysis was presented. As a result, the hybrid PV/WT/battery is proved more economical than using each system individually.

Xiao Xu et al. [19] designed and investigated a hybrid PV/WT/hydropower/pump storage as a case of study. The optimal configuration of the HRES is found using a techno-economic index that respects the maximum Loss of Power Supply Probability (LPSP) and minimum investment cost. The Multi-Objective Particle Swarm Optimization (MOPSO) is used to trade off analysis between two objectives. Besides, the curtailment rate (CR) of the WT and PV are taken into consideration due to policy requirements. The authors in [20] proposed an optimized design of an energy system featuring the highest penetration of renewable energy. This system is composed of WT, PV, geothermal, diesel, and BESS; otherwise, the system is obtained respecting the technological and financial feasibility constraints. The model developed is based on weather and electric demand data measured to reach the optimal sizing of the hybrid system. Three objective functions are conflicting, which are the Net Present Cost (NPC), renewable energy fraction and the energy index of reliability.

In [21], the authors implemented and compared three algorithms to find the optimal design of a hybrid WT/PV/Biomass/BESS energy system. Based on the obtained results, the Harmony Search Algorithm (HSA) was faster and efficient in the convergence, compared to Jaya and PSO optimization algorithms. The techno-economic study has been implemented to have the optimal unit sizing of the HRES, which guaranteed a cost-effective, efficient, and reliable power supply for the customers of electric energy. The constraints are chosen to enhance the reliability and efficiency of the hybrid system, using the LPSP and the energy fraction factors.

In this paper, a new smart algorithm named Bonobo Optimizer [22] was employed and improved using a quasi-oppositional method, and the modified Quasi Oppositional BO (QOBO) was utilized for optimal economic designing of a stand-alone microgrid hybrid system in Aswan, Egypt, where the hybrid system consists of RES (PV panels, WT and BESS) with diesel generators. Then, the results were

compared between the traditional and improved BO. This proved the ability of the QOBO algorithm to reach the optimal solution in a shorter time and with better efficiency compared to the traditional BO algorithm. Other algorithms, namely Harris Hawks Optimization, Artificial Electric Field Algorithm and Invasive Weed Optimization are applied, and the results are compared where the efficiency of the QOBO algorithm has been proved. Additionally, a sensitivity analysis of the proposed systems scenarios was performed to obtain the optimal solution.

2. Mathematical Description of the Proposed Hybrid System Components

The schematic diagram of the suggested HRES is shown in Figure 1. Four scenarios are applied, which include the PV power plant, WT power plant, diesel generator, Biomass, BESS and inverter.

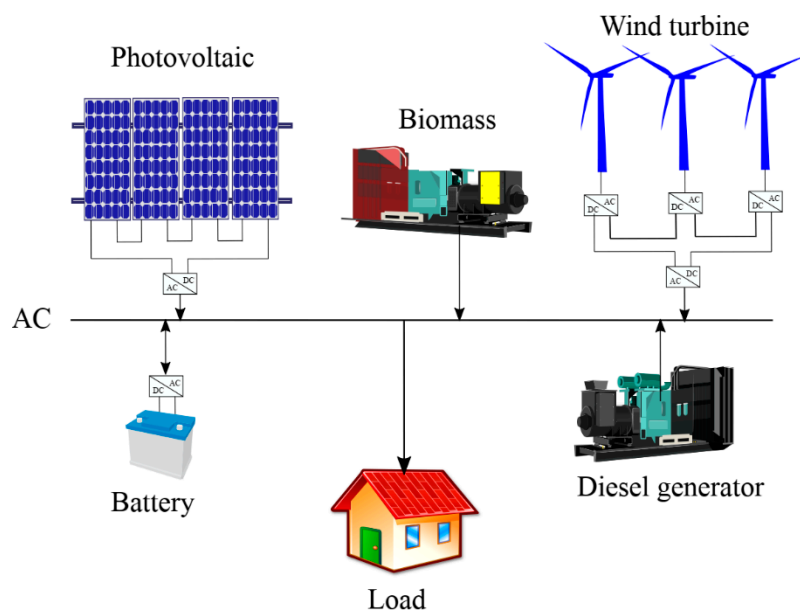


Figure 1. Configuration of the proposed microgrid hybrid energy system.

Two strategies are adopted in this paper; the first is the biomass/PV as shown in Figure 2 and the second uses the PV or WT or both as in Figure 3. The main strategy steps for the operation of the proposed system can be explained as follows:

- The PV and WT are used first as a principal power source and served the load needs.
- The battery is used when the PV and WT cannot serve it.
- The diesel system is working when the battery storage system is empty and starts when the need is higher than 30% of its nominal power.

2.1. PV System

The PV system is considered as a number of cells connected in series. The output power of the PV system is presented based on many parameters as introduced in Equation (1) [23]:

$$P_{pv} = I(t) \times \eta_{pv}(t) \times A_{pv} \tag{1}$$

where I represents the solar irradiation, A_{pv} represents the area covered with PV modules and η_{pv} is the efficiency of the PV system that can be calculated as follows:

$$\eta_{pv}(t) = \eta_r \times \eta_t \times \left[1 - \beta \times (T_a(t) - T_r) - \beta \times I(t) \times \left(\frac{NOCT - 20}{800} \right) \times (1 - \eta_r \times \eta_t) \right] \tag{2}$$

where $NOCT$ is the nominal operating cell temperature ($^{\circ}C$), η_r is the reference efficiency, η_t is the efficiency of the maximum power point tracking (MPPT) equipment, β is the temperature coefficient, T_a is the ambient temperature ($^{\circ}C$), T_r is the solar cell reference temperature ($^{\circ}C$).

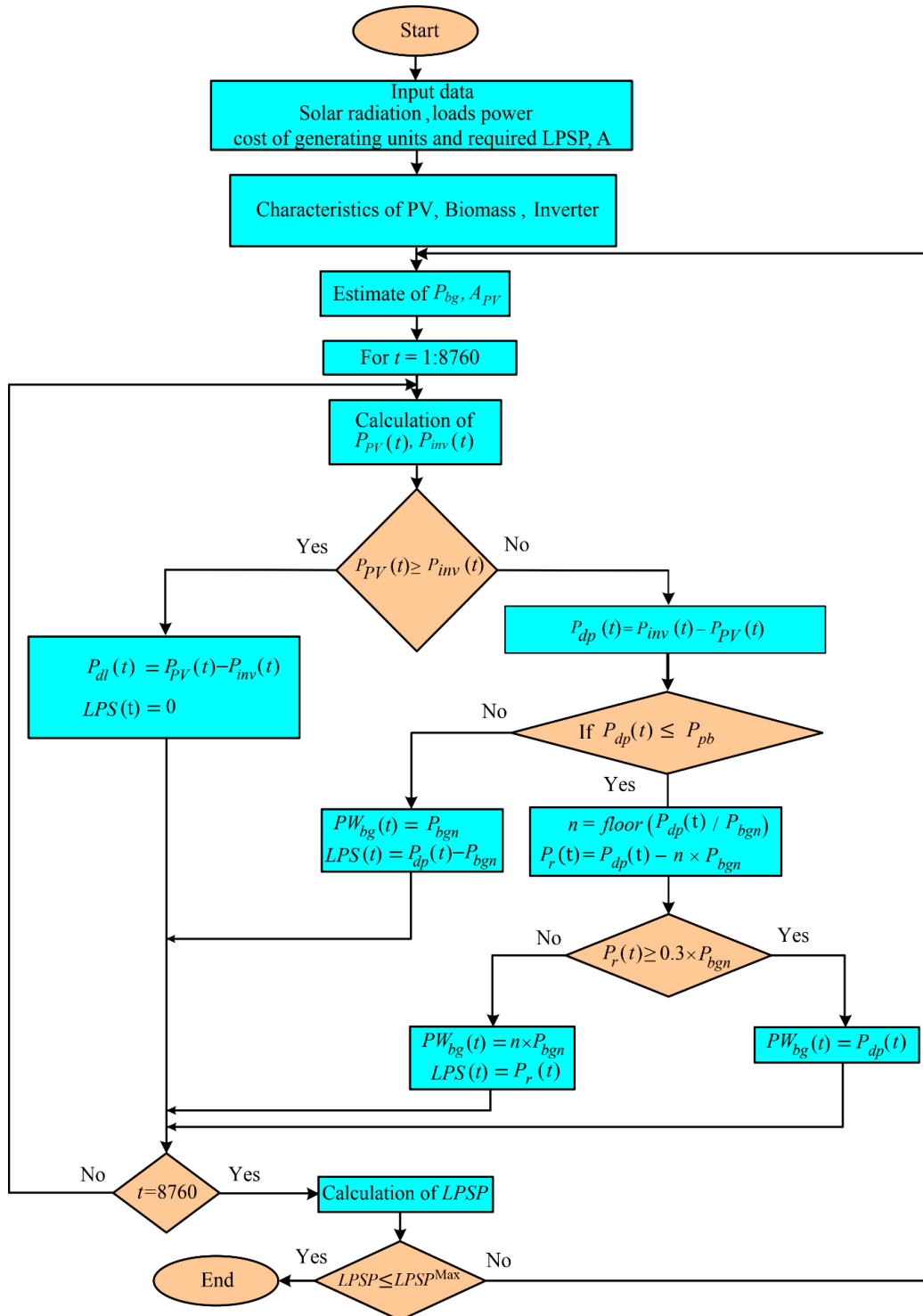


Figure 2. Power management of the PV/Biomass hybrid renewable energy sources (RES).

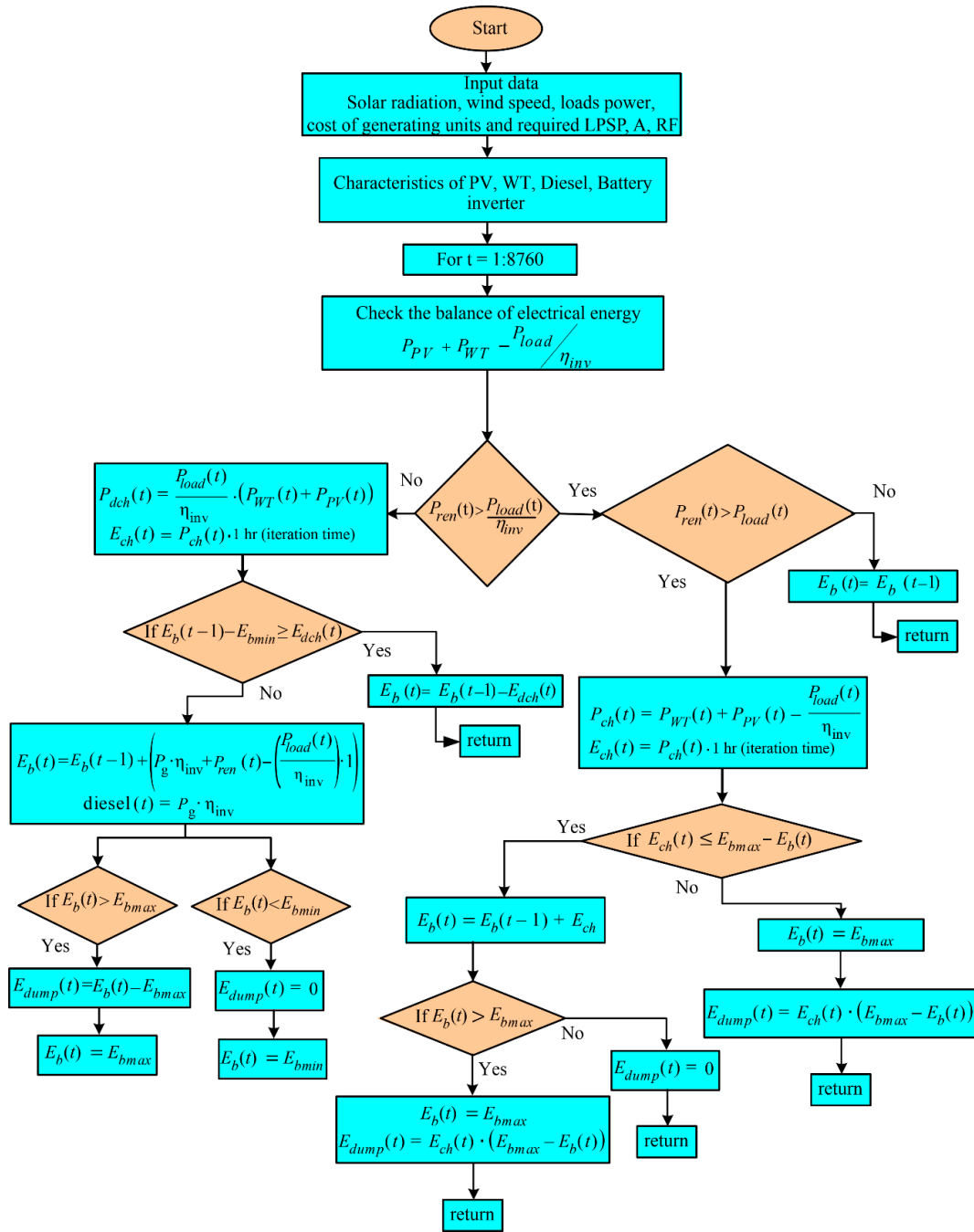


Figure 3. Power management of the PV/WT/diesel/battery energy storage system (BESS), PV/diesel/BESS and WT/diesel/BESS hybrid RES.

2.2. Wind Energy System

Based on the basics of aerodynamics, wind power can be presented as [24]:

$$P_{wind} = \begin{cases} 0, & V(t) \leq V_{ci}, V(t) \geq V_{co} \\ a \times V(t)^3 - b \times P_r, & V_{ci} < V(t) < V_r \\ P_r, & V_r \leq V(t) < V_{co} \end{cases} \quad (3)$$

where V represents wind speed, P_r is the rated power of wind, V_{ci} , V_{co} and V_r are the cut-in, cut-out, and rated wind speed, respectively. a and b are two constants, which can be expressed as:

$$\begin{cases} a = P_r / (V_r^3 - V_{ci}^3) \\ b = V_{ci}^3 / (V_r^3 - V_{ci}^3) \end{cases} \quad (4)$$

The rated power of wind is calculated as given in the following equation:

$$P_r = \frac{1}{2} \times \rho \times A_{wind} \times C_p \times V_r^3 \quad (5)$$

where ρ represents the air density, A_{wind} is the swept area of the wind turbine, C_p is the maximum power coefficient ranging from 0.25% to 0.45%.

2.3. Biomass System

The biomass system is a renewable energy system, which produces power as given in Equation (6) [23].

$$P_{BM} = \frac{Total_{bio} \times 1000 \times CV_{bio} \times \eta_{bio}}{8760 \times O_{time}} \quad (6)$$

where $Total_{bio}$ is the total organic material of biomass, CV_{bio} is the calorific value of the organic material (20 MJ/kg), η_{bio} is the biomass efficiency, which is taken as 24% and O_{time} presents the operating hours each day.

2.4. Diesel System

The diesel generator is used as a back-up, working just in case there is a need, is connected directly with the load, and starts when the battery is fully discharged and the load is more than 30% of its rated capacity. The model of the diesel generator regarding its output power is presented by the following Equation [25]:

$$P_{dg} = \frac{F_{dg}(t) - A_g \times P_{dg,out}}{B_g} \quad (7)$$

where F_{dg} is fuel consumption, $P_{dg,out}$ is the output power of diesel generator, A_g and B_g are the constants of the linear consumption of the fuel.

2.5. BESS System

The battery energy storage system (BESS) is a mandatory element for the isolated hybrid systems. BESS is charged in the periods of power excess and discharged when the load increases. The capacity of the BESS is expressed as follows [25]:

$$C_{bat} = \frac{E_l \times AD}{DOD \times \eta_{inv} \times \eta_b} \quad (8)$$

where E_l is the load demand, AD represents the autonomy daily of the battery, DOD is the depth of discharge of the battery system, η_{inv} and η_b are the battery and inverter efficiency, respectively.

3. Formulation of the Optimization Problem

3.1. Net Present Cost

The objective function in the optimization model is the minimization for the Net Present Cost (NPC) which is the pillar factor considered for any project design; it is counted as a sum of all components costs including the capital (C), operation and maintenance (OM) and replacement costs (R), considering also the fuel cost of the diesel (FC_{dg}), taking into account the interest rate (i_r), inflation

rate (δ), and escalation rate (μ) and the predefined project lifetime (N). The NPC modeling is expressed as follows [23,24]:

$$NPC = C + OM + R + FC_{dg} \tag{9}$$

3.1.1. PV and WT Costs

The costs of PV and WT are presented in a similar concept, their capital cost is expressed based on its initial cost ($\lambda_{PV,WT}$) and its area ($A_{PV,WT}$), the capital cost is as follows [26]:

$$C_{PV,WT} = \lambda_{PV,WT} \times A_{PV,WT} \tag{10}$$

The operation and maintenance costs are expressed as [26]:

$$OM_{PV,WT} = \theta_{PV,WT} \times A_{PV,WT} \times \sum_{i=1}^N \left(\frac{1 + \mu}{1 + i_r} \right)^i \tag{11}$$

where $\theta_{PV,WT}$ is the annual operation and maintenance costs for any components. The replacement costs are considered null because the project lifetime and the PV or WT lifetime are the same.

3.1.2. Diesel Generator Costs

The costs of the diesel generator are presented as follows [27]:

$$C_{dg} = \lambda_{dg} \times P_{dg} \tag{12}$$

$$OM_{dg} = \theta_{dg} \times N_{run} \times \sum_{i=1}^N \left(\frac{1 + \mu}{1 + i_r} \right)^i \tag{13}$$

$$R_{diesel} = R_{dg} \times P_{dg} \times \sum_{i=7,14,\dots} \left(\frac{1 + \delta}{1 + i_r} \right)^i \tag{14}$$

$$C_f(t) = p_f \times F_{dg}(t) \tag{15}$$

$$FC_{dg} = \sum_{t=1}^{8760} C_f(t) \times \sum_{i=1}^N \left(\frac{1 + \delta}{1 + i_r} \right)^i \tag{16}$$

where C_{dg} is the capital cost, λ_{dg} is the initial cost of the diesel generator for each KW, OM_{dg} represent the actual O&M cost, θ_{dg} is the annual O&M cost of diesel, N_{run} is the number of operating hours of diesel generator per year, R_{diesel} is the diesel generator replacement cost, R_{dg} represents the annual replacement cost of diesel generator, p_f is the fuel cost, F_{dg} is the annual consumption of fuel and FC_{dg} is the total fuel cost.

3.1.3. BESS Costs

The capital and O&M (containing the replacement) costs of the BESS are expressed as follows [26]:

$$C_{BESS} = \lambda_{bat} \times C_{bat} \tag{17}$$

$$OM_{BESS} = \theta_{bat} \times C_{bat} \times \sum_{i=1}^{T_B} \left(\frac{1 + \mu}{1 + \delta} \right)^{(i-1)N_{bat}} \tag{18}$$

where λ_{bat} is the BESS initial cost and θ_{bat} is the annual O&M cost of BESS.

3.1.4. Biomass Costs

The biomass costs are presented as follows [28]:

$$C_{bg} = \lambda_{bg} \times P_{bg} \tag{19}$$

$$OM_{bg} = \theta_1 \times P_{bg} \times \sum_{i=1}^N \left(\frac{1 + \mu}{1 + i_r} \right)^i + \theta_2 \times P_w \times \sum_{i=1}^N \left(\frac{1 + \mu}{1 + i_r} \right)^i \quad (20)$$

where λ_{bg} is the biomass initial cost, θ_1 is the annual fixed O&M cost and θ_2 is the variable O&M cost of the biomass system, and P_w is the annual energy generated by the Biomass system (kWh/Year).

3.1.5. Inverter Costs

The inverter capital and O&M costs are presented as follows [27]:

$$C_{inv} = \lambda_{inv} \times P_{inv} \quad (21)$$

$$OM_{Inv} = \theta_{Inv} \times \sum_{i=1}^N \left(\frac{1 + \mu}{1 + i_r} \right)^i \quad (22)$$

where λ_{inv} is the inverter initial cost and θ_{Inv} is the annual O&M cost of the inverter.

3.2. Levelized Cost of Energy

The Levelized Cost of Energy (LCOE) is a critical factor. The consumers do not care about project cost or its lifetime, but their interest is to know how much to pay for each kilowatt-hour of consumption. Therefore, the LCOE is a measure of the average NPC over its lifetime, its equation is expressed as follows [25]:

$$LCOE = \frac{NPC \times CRF}{\sum_{t=1}^{8760} P_{load}(t)} \quad (23)$$

where P_{load} is the load demand; CRF is the capital recovery factor used to convert the initial cost to an annual capital cost, and is expressed as follow:

$$CRF(i_r, R) = \frac{i_r \times (1 + i_r)^R}{(1 + i_r)^R - 1} \quad (24)$$

where R denotes the lifetime of the hybrid system.

3.3. Loss of Power Supply Probability

The loss of power supply probability (LPSP) is a technical factor used to express the reliability of the system. The LPSP is expressed as follows [25]:

$$LPSP = \frac{\sum_{t=1}^{8760} (P_{load}(t) - P_{pv}(t) - P_{wind}(t) + P_{dg,out}(t) + P_{bmin})}{\sum_{t=1}^{8760} P_{load}(t)} \quad (25)$$

3.4. Renewable Energy Fraction

The transfer from classical electricity production to renewable energy projects was not easy. The majority introduced RES partially, while the objective is to use all projects with 100% renewable energy. Therefore, the renewable energy factor is dedicated to calculating the percentage of the renewable energy used. The renewable energy fraction (RF) is expressed as follows [25]:

$$RF = \left(1 - \frac{\sum_{t=1}^{8760} P_{dg,out}(t)}{\sum_{t=1}^{8760} P_{re}(t)} \right) \times 100 \quad (26)$$

where P_{re} represents the total power from RES.

3.5. Availability Index

The availability index (A) is calculated to predict customer satisfaction. The availability index measures the energy converted to the load while confirming the ability of the designing system of the project. The availability index is calculated as follows [23]:

$$A = 1 - \frac{DMN}{\sum_{t=1}^{8760} P_{load}(t)} \quad (27)$$

$$DMN = P_{bmin}(t) - P_b(t) - (P_{pv}(t) + P_{wind}(t) + P_{dg,out}(t) - P_{load}(t)) \times u(t) \quad (28)$$

while, u will be equal to 1 when the load is not satisfied, and 0 when the load is satisfied.

3.6. Constraints

The constraints are presented to achieve the desired system design. In this microgrid system, the constraints are shown as follows:

$$\begin{aligned} 0 &\leq A_{pv} \leq A_{pv}^{max}, \\ 0 &\leq A_{wind} \leq A_{wind}^{max}, \\ 0 &\leq P_{dgn} \leq P_{dgn}^{max}, \\ 0 &\leq P_{Cap_bat} \leq P_{Cap_bat}^{max}, \\ LPSP &\leq LPSP^{max}, \\ RF^{min} &\leq RF, \\ A^{min} &\leq A \\ AD^{min} &\leq AD \end{aligned} \quad (29)$$

4. Algorithms

In this section, the conventional BO and proposed QOBO are illustrated. In addition, both algorithms are compared with well-known optimization techniques (HHO, AEFA and IWO) which are briefly described in Appendix A.

4.1. Bonobo Optimizer

Bonobo optimizer is a new optimization algorithm that was proposed in [22]. In BO, the social reproductive behavior of the bonobo is modeled based on four mating strategies: promiscuous, restrictive, consortship, and extra-group mating. These mating strategies are subjected to the living condition of the bonobo, hence two terms named positive phase (PP) and negative phase (NP) have been used to present the situations of this life. In this framework, PP describes the peaceful living in which the mating can be done. On the contrary, NP expresses a hard life. In the BO, each solution is called X_B and the best solution is X_B^α . The mathematical modeling of the BO algorithm is presented in the following subsections.

4.1.1. Bonobo Selection Using Fission–Fusion Strategy

The solutions update of the BO algorithm depends on the mating strategies subjected to the current phase. However, a bonobo should be selected before each mating based on the fission–fusion social group strategy. As noted, the bonobo community lives in small groups with different sizes (random and unpredictable) for a few days and the communities rejoined again to the main community. Hence, based on this behavior, a bonobo for mating can be selected. The mathematical formulation for the maximum number of these temporary subgroups N_{sub} can be expressed as follows:

$$N_{sub} = \max(2, (\varepsilon_{sub} \times N)) \quad (30)$$

where N is the total number of the population and ε_{sub} denotes the sub-group size factor. To find the selected bonobo X_B^P for mating with X_B^i to create a new bonobo X_B^{new} , if the best bonobo in the subgroup in terms of the fitness function is better than the X_B^i , then it is selected as X_B^P , else a random one should be selected from the subgroup.

4.1.2. Creation of New Bonobo

After achieving the selected bonobo X_B^P , four mating strategies are used in the BO algorithm to create a new bonobo X_B^{new} based on the current phase (PP or NP). For the PP case, promiscuous and restrictive mating have higher probabilities (ρ_{ph}) for occurrence. On the contrary, in NP, the probabilities (ρ_{ph}) of consortship mating and extra-group mating are higher.

Promiscuous and Restrictive Mating

In this mating strategy, the new bonobo can be created using the following equation:

$$X_B^{new} = X_B^i + r_1 \times S_{coef}^\alpha \times (X_B^\alpha - X_B^i) + (1 - r_1) \times S_{coef}^P \times C_{flag} \times (X_B^i - X_B^P) \tag{31}$$

where r_1 is a random number between $[0, 1]$. S_{coef}^α and S_{coef}^P are the sharing coefficients for the alpha bonobo X_B^α and the selected bonobo X_B^P , respectively. C_{flag} is a flag value that equals -1 or 1 for restrictive and promiscuous mating, respectively. A controlling parameter in terms of the phase probability ρ_{ph} is used to adopt the mating strategy. Initially, ρ_{ph} is set to 0.5 . Hence, if a random number r is found to be less than or equal to ρ_{ph} , a new bonobo is created based on promiscuous and restrictive mating, otherwise, consortship mating and extra-group mating can be used.

Consortship and Extra-Group Mating

If r is greater than ρ_{ph} , consortship and extra-group mating can occur. However, a new random number r_2 between $[0, 1]$ is used with a probability of extra-group mating ρ_{xg} to represent the occurrence of extra-group mating when r_2 is less than or equal to ρ_{xg} as follows [22,29]:

$$X_B^{new} = \begin{cases} X_B^i + \beta_1 \times (X_{max}^i - X_B^i), & X_B^\alpha \geq X_B^i, \text{ and } r_4 \leq \rho_d \\ X_B^i - \beta_2 \times (X_B^i - X_{min}^i), & X_B^\alpha \geq X_B^i, \text{ and } r_4 > \rho_d \\ X_B^i - \beta_1 \times (X_B^i - X_{min}^i), & X_B^\alpha < X_B^i, \text{ and } r_4 \leq \rho_d \\ X_B^i + \beta_2 \times (X_{max}^i - X_B^i), & X_B^\alpha < X_B^i, \text{ and } r_4 > \rho_d \end{cases} \tag{32}$$

$$\beta_1 = e^{(r_4^2 + r_4 - \frac{2}{r_4})} \tag{33}$$

$$\beta_2 = e^{(-r_4^2 + 2r_4 - \frac{2}{r_4})}$$

where r_3 and r_4 are random numbers between $[0, 1]$ and $r_4 \neq 0$. ρ_d is a directional probability with initial value which equals 0.5 . β_1 and β_2 are intermediate parameters between $[0, 1]$. X_{min}^i and X_{max}^i are the values of the upper and lower boundary.

If r_2 is greater than ρ_{xg} , a new bonobo can be created using the consortship mating strategy as follows:

$$X_B^{new} = \begin{cases} X_B^i + C_{flag} \times e^{-r_5} \times (X_B^i - X_B^P), & C_{flag} = 1 \text{ or } r_6 \leq \rho_d \\ X_B^P, & \text{Otherwise} \end{cases} \tag{34}$$

where r_5 and r_6 are two random numbers.

4.1.3. Parameter Updating

The BO's parameters are updated during the iterative process based on the best solution X_B^α at each iteration, where if there is an improvement in the final solution compared to the previous iteration, the BO's parameters can be updated in the following way.

The negative phase count is set to zero ($NP_{cont} = 0$) and the positive phase count grows by increments of one ($PP_{cont} = PP_{cont} + 1$). In addition, $\rho_{xg} = \rho_{xg_initial}$ and $\rho_{ph} = 0.5 + Cp$ where Cp is the amount of the change in the phase, and can be calculated as $Cp = \min(0.5, PP_{cont} \times rcp)$ where rcp is the rate of the change in the phase. Moreover $\rho_d = \rho_{ph}$ and

$$\epsilon_{sub} = \min(\epsilon_{sub_max}, (\epsilon_{sub_initial} + PP_{cont} \times rcp^2)) \tag{35}$$

where $\epsilon_{sub_initial} = 0.5 * \epsilon_{sub_max}$.

On the other hand, if there is no improvement, the BO's parameters are updated as follows:

$$\begin{aligned} NP_{cont} &= NP_{cont} + 1 \text{ and } PP_{cont} = 0, \\ Cp &= \min(0.5, NP_{cont} \times rcp), \\ \rho_{xg} &= \rho_{xg_initial} \min(0.5, \rho_{xg_initial} + NP_{cont} \times rcp^2), \\ &\text{and} \\ \epsilon_{sub} &= \min(\epsilon_{sub_max}, (\epsilon_{sub_initial} - NP_{cont} \times rcp^2)). \end{aligned}$$

The overall steps of the BO algorithm are presented in Algorithm 1.

Algorithm 1: BO

Initialize a set of random search bonobo $X_B^i = (X_B^1, X_B^2, \dots, X_B^N)$ within the limits $X_{min}^i \leq X_B^i \leq X_{max}^i$.
 Initialize the BO's parameters
 Evaluate the objective function for all bonobos
 Identify the alpha bonobo X_B^α
 While ($k < K_{max}$)
 Determine the actual size of the temporary sub-group
 Choose a bonobo using fission-fusion society strategy
 Create a new bonobo X_B^{new} as follows:
 if $r \leq \rho_{ph}$
 Create new bonobo using promiscuous or restrictive mating strategy
 else $r > \rho_{ph}$
 Create new bonobo using consortship or extra-group mating strategy
 end if
 Calculate the objective function
 Update alpha bonobo X_B^α and the BO's parameters.
 $K = K + 1$
 end while
 Return the final best solution X_B^α

4.2. Improved Quasi-Oppositional BO (QOBO) Algorithm

As with any population-based algorithm, BO has some problems such as falling in the local optima. However, in this work, an improved BO based on three leaders' selection and quasi-opposition-based learning is developed.

4.2.1. Three Leaders

In this method, instead of using the best solution (alpha bonobo X_B^α) for updating the new bonobo X_B^{new} and ignoring the other best solutions, three leaders can be used to increase the diversity of the solutions as follows

$$X_B^\alpha = w_1 \times X_{best_1} + w_2 \times X_{best_2} + w_3 \times X_{best_3} \tag{36}$$

where

$$w_1 = \frac{r_7}{r_7 + r_8 + r_9}, w_2 = \frac{r_8}{r_7 + r_8 + r_9}, \text{ and } w_3 = \frac{r_9}{r_7 + r_8 + r_9}$$

$r_7, r_8,$ and r_9 are random values between $[0, 1]$.

4.2.2. Quasi-Oppositional

Opposition-based learning (OBL) [30] has been widely used to improve many optimization techniques such as quasi-oppositional teaching-learning (QOTLBO) [31,32], Quasi-oppositional swine influenza model-based optimization with quarantine (QOSIMBO-Q) [33] and Oppositional Jaya Algorithm [34]. In the OBL, improvements can be achieved by using the candidate solution and its opposite at the same time. Hence, in this work, the opposite solution of the BO algorithm X_B^i can be expressed as presented in [35]:

$$X_B^{qnew} = C + r_{10}(C - \overline{X_B^{new}}) \tag{37}$$

where r_{10} is a random number between [0, 1], and C is a middle point between X_{min}^i and X_{max}^i which can be calculated as follows:

$$C = \frac{X_{min}^i + X_{max}^i}{2} \tag{38}$$

Additionally, $\overline{X_B^{new}}$ is the opposite solution which can be calculated as

$$\overline{X_B^{new}} = X_{min}^i + X_{max}^i - X_B^{new} \tag{39}$$

The overall steps of the improved BO based on three leaders and the quasi-oppositional method are presented in Algorithm 2.

Algorithm 2: QOBO

Initialize a set of random search bonobo $X_B^i = (X_B^1, X_B^2, \dots, X_B^N)$ within the limits $X_{min}^i \leq X_B^i \leq X_{max}^i$.

Initialize the BO's parameters

Evaluate the objective function for all bonobos

Determine the alpha bonobo X_B^α using three-leader method

While ($k < K_{max}$)

 Determine the actual size of the temporary sub-group

 Choose a bonobo using fission-fusion society strategy

 Create a new bonobo X_B^{new} as follows:

 if $r \leq \rho_{ph}$

 Create new bonobo using promiscuous or restrictive mating strategy

 else $r > \rho_{ph}$

 Create new bonobo using consortship or extra-group mating strategy

 end if

 Calculate the objective function for all new bonobos X_B^{new}

 Find quasi-oppositional model for all new bonobos X_B^{qnew}

 Calculate the objective function for all new bonobos X_B^{qnew}

 if $f(X_B^{qnew}) \leq f(X_B^{new})$, $X_B^{new} = X_B^{qnew}$

 Else $X_B^{new} = X_B^{new}$

 end if

 Update alpha bonobo X_B^α using three leader method and the BO's parameters.

$K = K + 1$

 end while

 Return the final best solution X_B^α

5. Case Study

To validate the robustness of the QOBO algorithm, it has been applied for addressing the studied problem of optimal configuration of the proposed multiple scenarios HRES, i.e., the PV/WT/diesel generator/BESS, PV/biomass, PV/diesel generator/BESS and WT/diesel generator/BESS. The proposed hybrid systems have been introduced in the isolated mode for satisfying the load requirements in the proposed site.

The project is applied in Aswan, Egypt as shown in Figure 4. The annual load curve over a time interval of one hour is shown in Figure 5. Figures 6–9 present solar irradiation, temperature, wind speed and atmospheric pressure in the studied region. Four standalone scenarios of the hybrid system will be evaluated for covering the load demand in that site. These configurations are: (1) PV/WT/diesel/BESS, (2) PV/biomass, (3) PV/diesel/BESS and (4) WT/diesel/BESS. The proposed QOBO is validated on optimal sizing of these four hybrid systems and the optimization results are comprehensively compared with the corresponding ones obtained from BO, HHO, AEFA and IWO algorithms.

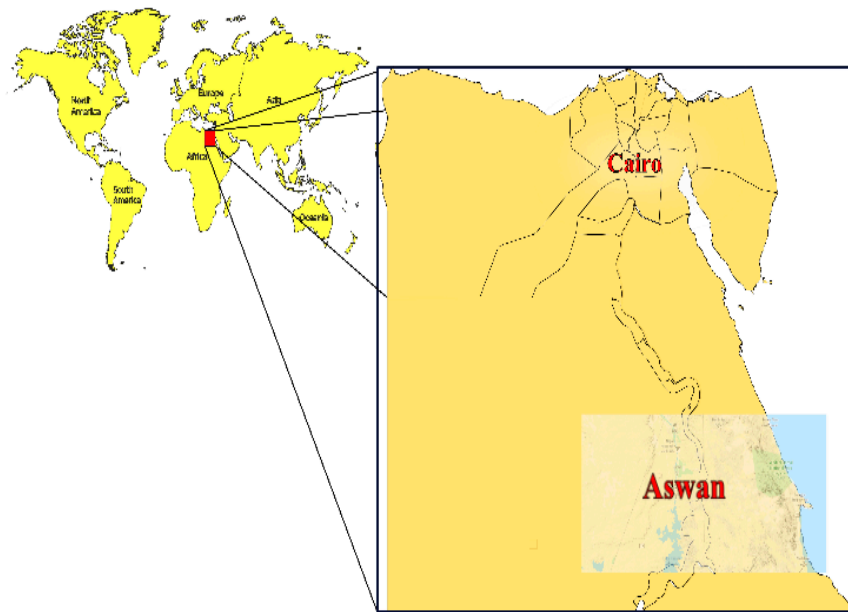


Figure 4. Location of the case study (Aswan) on the world map.

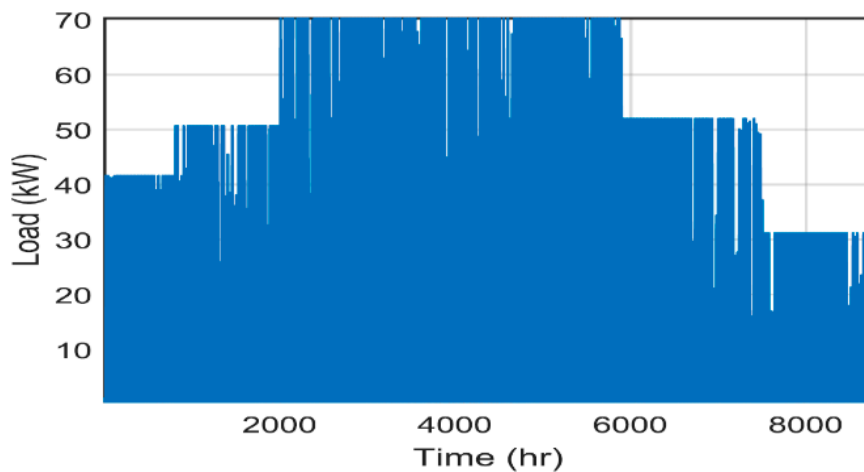


Figure 5. Annual load curve over a time interval of one hour with a peak demand of 70 kW.

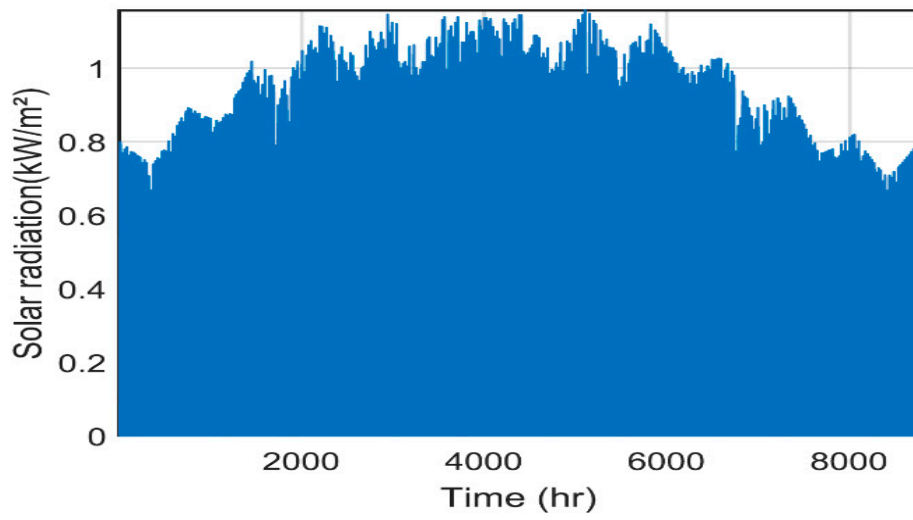


Figure 6. Solar irradiation over the studied region.

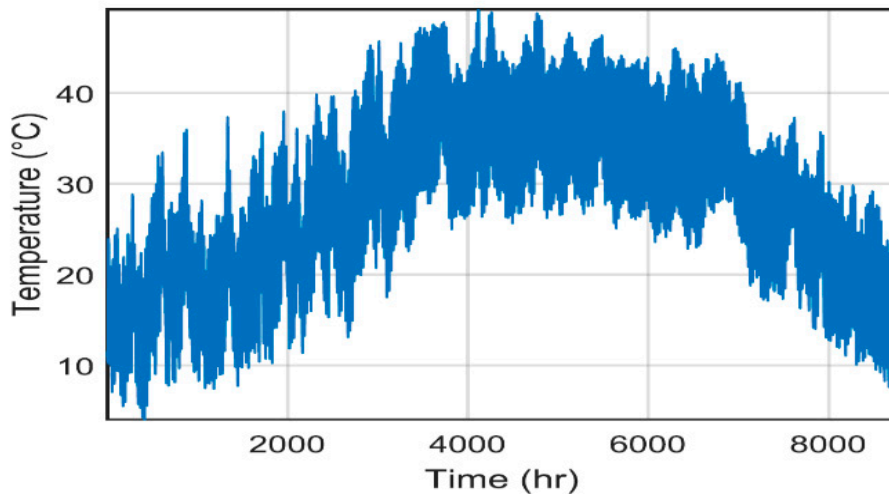


Figure 7. Temperature variation in Aswan.

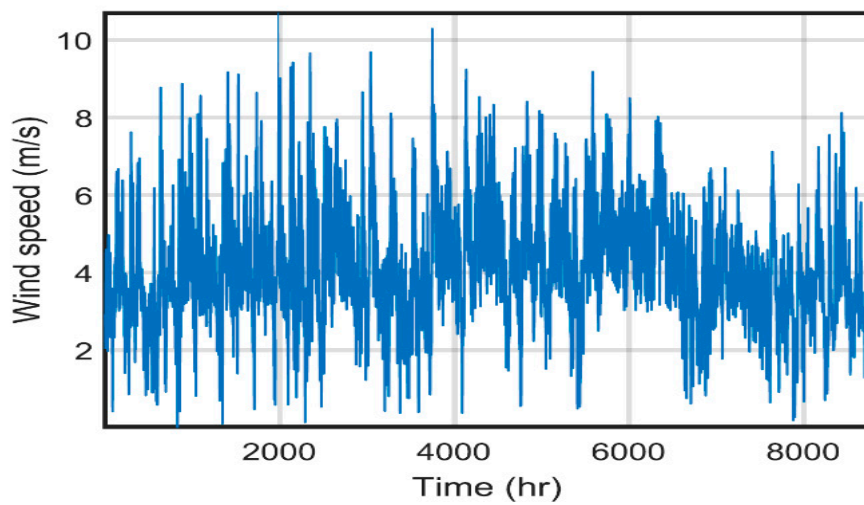


Figure 8. Annual variation of wind speed over the year in Aswan.

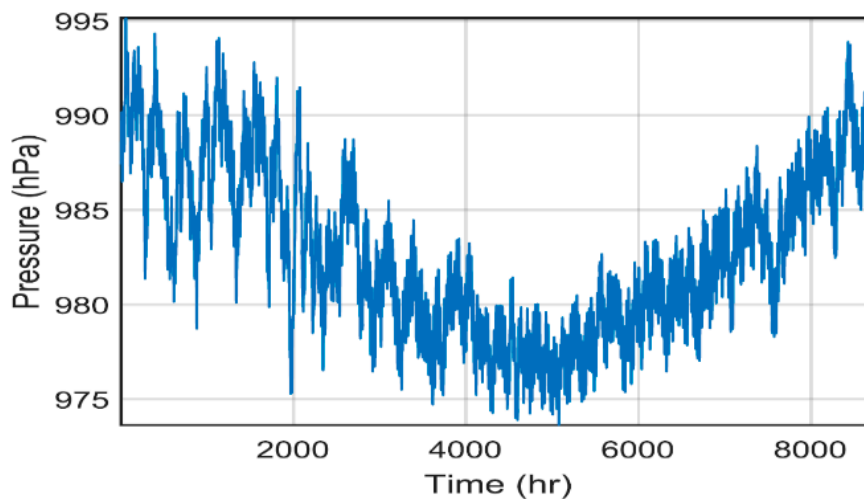


Figure 9. Atmospheric pressure variation in Aswan.

6. Results

The main object of this research paper is to find the optimal design of the proposed hybrid system and to validate the accuracy of the proposed QOBO optimization method. The optimal sizing is based on the objective functions introduced in (9) and the parameters of optimization are: (i) the area of PV system, (ii) the area swept by the WT, (iii) the rated power of diesel generator, (iv) the nominal capacity of the battery, (v) the consumption of the biomass fuel. To confirm the suitability of the QOBO in addressing such optimization problem, QOBO, BO, HHO, AEFA and IWO were launched 100 times for each configuration and statistical study was conducted based on the best minimum value of the fitness function. For a deep analysis of the obtained results and to ensure the sensitivity analysis, four indices were chosen, namely, NPC, LCOE, LPSP and the availability index. In the next subsections, the optimization results are provided for the standalone system with multiple scenarios. Modelling and simulation of the optimization problem were accomplished using MATLAB 2015a program, while the adjusting parameters for the three algorithms are the same, i.e., the number of maximum iterations is taken as 100 iterations and the search agents' number is 30 agents. The input technical and economic data for the system components are presented in Table 1. The results of the statistical measurements for the modified QOBO and the conventional BO with HHO, AEFA and IWO algorithms are listed in Tables 2 and 3. From the previously mentioned tables, the reader can conclude that the QOBO technique generates the best minimum value of the fitness function in all cases. The convergence curves of the 100 iterations implemented for all the studied configurations using QOBO, BO, HHO, AEFA and IWO are presented in Figure 10a–d.

Table 1. Units for magnetic properties.

Symbol	Quantity	Conversion
N	Project lifetime	20 years
i_r	Interest rate	13.25%
μ	Escalation rate	2%
δ	Inflation rate	12.27%
PV system		
λ_{pv}	PV initial cost	300 \$/m ²
θ_{pv}	Annual O&M cost of PV	$0.01 * \lambda_{pv}$ \$/m ² /year
η_r	Reference efficiency of the PV	25%
η_t	Efficiency of MPPT	100%
T_r	PV cell reference temperature	25 °C
β	Temperature coefficient	0.005 °C
NOCT	Nominal operating cell temperature	47 °C
N_{pv}	PV system lifetime	20 years
WT system		
λ_{wind}	Wind initial cost	125 \$/m ²
θ_{wind}	Annual O&M cost of wind	$0.01 * \lambda_{wind}$ \$/m ² /year
C_{p_wind}	Maximum power coefficient	48%
V_{ci}	Cut-in wind speed	2.6 m/s
V_{co}	Cut-out wind speed	25 m/s
V_r	Rated wind speed	9.5 m/s
N_{wind}	Wind system lifetime	20 years
Diesel generator		
λ_{dg}	Diesel initial cost	250 \$/kW
θ_{dg}	Annual O&M cost of diesel	0.05 \$/h
R_{dg}	Replacement cost	210 \$/kW
p_f	Fuel price in Egypt	0.43 \$/L
N_{diesel}	Diesel system lifetime	7 years
BESS		
λ_{bat}	Battery initial cost	100 \$/kWh
θ_{bat}	Annual operation and maintenance cost of battery	$0.03 * \lambda_{bat}$ \$/m ² /year
DOD	Depth of discharge	80%
η_b	Battery efficiency	97%
SOC _{min}	Minimum state of charge	20%
SOC _{max}	Maximum state of charge	80%
N_{bat}	Battery system lifetime	5 years
Inverter		
λ_{inv}	Inverter initial cost	400 \$/m ²
θ_{inv}	Annual O&M cost of inverter	20 \$/year
η_{inv}	Inverter efficiency	97%

6.1. Validation of QOBO Algorithm

The results of the statistical measurements for the modified QOBO, the conventional BO, HHO, AEFA and IWO algorithms are listed in Tables 2 and 3. From Table 2, the reader can find the results of the optimal sizing for the multiple scenarios studied, as well as the convergence time of each simulation, and conclude that the QOBO algorithm finds the best results with a short time compared with the other algorithms. From Table 3, the reader can compare between algorithms and the different scenarios of the proposed hybrid system using multiple factors. Briefly, it is noticed that the hybrid PV/biomass system is highly competitive, mainly using the developed QOBO algorithm, the optimized system is calculated with \$110,807, which means an LCOE of 0.1053 \$/kWh, the constraints are satisfied and the project is 100% supplied by renewable energy sources. In this scenario, the performances of the QOBO and the BO are almost equal, while in other scenarios, the difference is clearly noticed.

Table 2. Sizing results of different scenarios obtained from different optimization methods.

Hybrid Power System	Algorithm	PV (m ²)	Wind (m ²)	Diesel (kW)	Battery (kWh)	Biomass (t/year)	Time(s)
PV/WT/Diesel/BESS	QOBO	484.765	0	1.2142	13.4390	//	51,507
	BO	248.002	998.505	0.6480	14.8052	//	164,242
	HHO	513.105	305.293	0.5204	14.6552	//	30,655
	AEFA	329.159	176.277	5.4696	18.6552	//	10,531
	IWO	830.791	136.557	10.296	5.8224	//	57,938
PV/Biomass	QOBO	293.971	//	//	//	1020.18	32,104
	BO	293.972	//	//	//	1020.31	122,417
	HHO	298.860	//	//	//	2040.47	10,453
	AEFA	302.980	//	//	//	1185.76	3855
	IWO	365.515	//	//	//	2739.00	36,098
PV/Diesel/BESS	QOBO	376.011	//	1.3402	58.9083	//	16,799
	BO	336.253	//	2.9170	52.1928	//	33,009
	HHO	482.756	//	1.7843	13.7590	//	13,983
	AEFA	386.692	//	1.6713	55.7583	//	6237
	IWO	748.387	//	4.0111	51.4565	//	24,630
WT/Diesel/BESS	QOBO	//	2726.29	91.141	72.375	//	26,510
	BO	//	2823.34	42.637	72.371	//	66,514
	HHO	//	2808.76	74.565	73.230	//	135,097
	AEFA	//	3015.08	72.963	72.653	//	78,697
	IWO	//	4318.76	78.218	82.7987	//	26,960

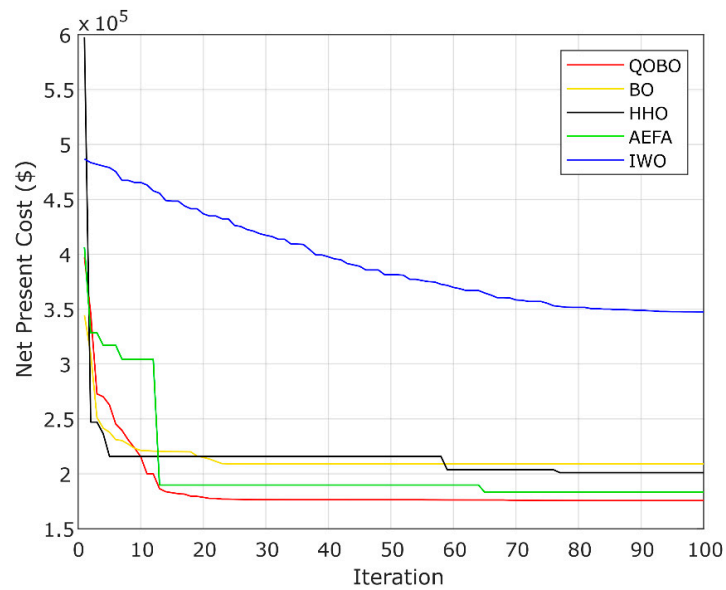
Table 3. Factor results for all scenarios.

Hybrid Power System	Algorithm	NPC (\$)	LCOE (\$/kWh)	LPSP (%)	Availability (%)	Renewable Energy (%)	Battery Daily Autonomy (day)
PV/WT/Diesel/BESS	QOBO	175,651	0.1669	0.019	98.87	98.15	0.5826
	BO	209,096	0.1986	0.050	96.99	99.75	0.6418
	HHO	201,109	0.1910	0.025	99.23	99.88	0.6353
	AEFA	183,284	0.1741	0.026	99.33	96.88	0.8087
	IWO	347,523	0.3301	0.014	99.68	97.72	0.2524
PV/Biomass	QOBO	110,807	0.1053	0.050	96.03	100	//
	BO	110,808	0.1053	0.050	96.03	100	//
	HHO	114,098	0.1084	0.046	96.94	100	//
	AEFA	113,410	0.1077	0.040	96.93	100	//
	IWO	130,491	0.1240	0.018	98.70	100	//
PV/Diesel/BESS	QOBO	153,401	0.1457	0.049	98.63	97.25	2.5536
	BO	167,981	0.1596	0.050	98.72	92.88	2.2625
	HHO	183,501	0.1743	0.017	98.94	97.27	0.5964
	AEFA	160,774	0.1527	0.042	98.74	96.70	2.4171
	IWO	287,730	0.2733	0.026	99.16	96.12	2.2306
WT/Diesel/BESS	QOBO	1,095,270	1.0405	0.014	99.85	70.03	3.9509
	BO	1,098,685	1.0437	0.003	99.97	71.3527	1.8483
	HHO	1,123,579	1.0673	0.008	99.92	70.2407	3.1745
	AEFA	1,119,533	1.0635	0.008	99.92	73.6967	3.1494
	IWO	1,319,108	1.2531	0.008	99.92	81.8292	3.3907

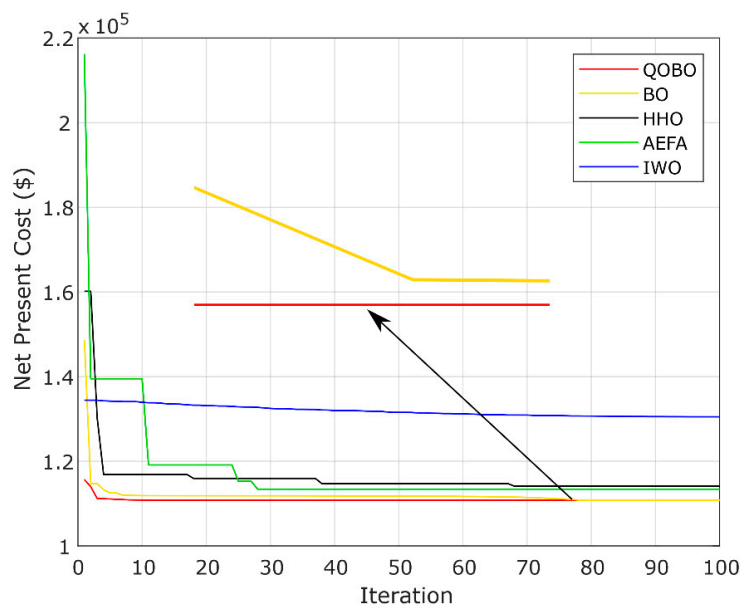
6.2. Combinations of the Studied System Components

In this section, the results obtained in the convergence simulation of the NPC as a fitness function using the QOBO are presented. The optimized parameter results (i.e., A_{pv} , A_{wind} , P_{dgn} , P_{Cap_bat} , P_{BM}) for all suggested combinations are listed in Table 3 with the rating of the inverter that takes the value of the peak load demand. From Figure 10, the reader can notice that using QOBO, BO, HHO, AEFA and IWO algorithms, the best minimum values of fitness function (NPC) is obtained for the second configuration, i.e., hybrid PV/biomass energy system. From the table, it is obvious that QOBO generates the minimum value of LCOE in all cases.

The reliability of the proposed scenarios of the proposed HRES are respected and the availability of power is highly assured, the penetration RES is considered in this paper, while different results are obtained. The minimum penetration of 70% is obtained for the WT/Diesel/Battery scenario while the maximum penetration of 99.75% is obtained for the PV/WT/Diesel/BESS scenario. The daily battery autonomy is also influenced by the configuration of the HRES, the best autonomy is achieved for the WT/Diesel/BESS scenario taking nearly 4 days, while the minimum autonomy is obtained in PV/WT/Diesel/BESS case with only 6 h. The last system is composed of the different energy resource which explains the independence for a specific resource. Table 4 presents a detailed overview of all costs needed, for all scenarios presented and for all proposed algorithms.



(a)



(b)

Figure 10. Cont.

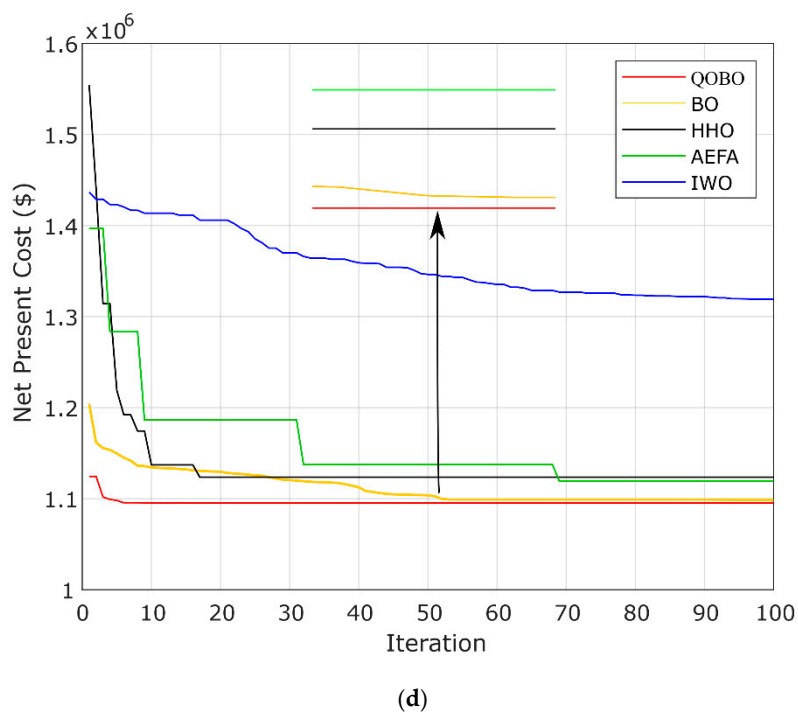
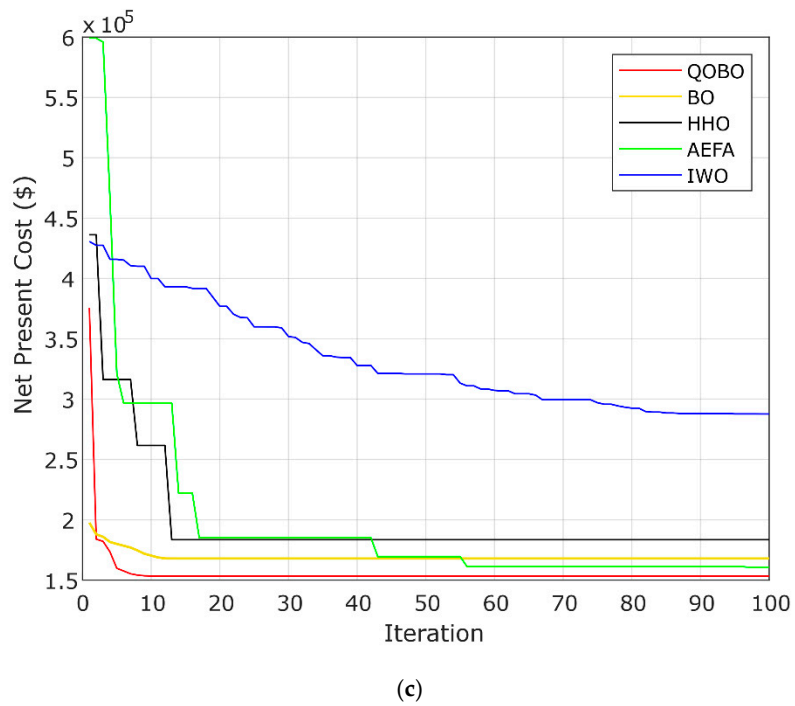


Figure 10. Convergence of the objective function of all algorithms for different scenarios; (a) PV/WT/Diesel/BESS, (b) PV/Biomass, (c) PV/Diesel/BESS, (d) WT/Diesel/BESS.

Table 4. Convergence of objective function of different scenarios.

Hybrid Power System	Algorithm	PV			Wind			Diesel			Battery			Inverter		Biomass		
		Costs	Inv	O&M	Rep	Inv	O&M	Rep	Inv	O&M	Rep	Fuel	Inv	Rep	Inv	Rep	Inv	O&M
Scenario I	QOBO	145,429	11,558	0	0	0	0	303	1792	465	17,080	1343	90	28,400	158			//
	BO	74,400	5913	0	124,813	9920	0	162	526	248	5244	1480	99	28,400	158			//
	HHO	153,931	12,234	0	38,161	3033	0	130	330	199	3729	1465	98	28,400	158			//
	AEFA	98,747	7848	0	22,034	1751	0	1367	537	2097	44,542	1865	125	28,400	158			//
	IWO	249,237	19,809	0	17,069	1356	0	2574	470	3949	80,625	582	39	28,400	158			//
Scenario II	QOBO	88,191	7009	0	//	//	//	//	//	//	//	//	//	28,400	158	1040	103	4696
	BO	88,191	7009	0	//	//	//	//	//	//	//	//	//	28,400	158	1040	103	4696
	HHO	89,658	7126	0	//	//	//	//	//	//	//	//	//	28,400	158	2080	129	5907
	AEFA	90,894	7224	0	//	//	//	//	//	//	//	//	//	28,400	158	1208	105	4820
	IWO	109,654	8715	0	//	//	//	//	//	//	//	//	//	28,400	158	2792	97	4416
Scenario III	QOBO	112,803	8965	0	//	//	//	335	1869	514	19,339	5890	395	28,400	158			//
	BO	100,875	8017	0	//	//	//	729	1994	1118	43,812	5219	350	28,400	158			//
	HHO	144,826	11,510	0	//	//	//	446	1792	684	25,102	1375	92	28,400	158			//
	AEFA	116,007	9220	0	//	//	//	417	1855	641	24,008	5575	374	28,400	158			//
	IWO	224,516	17,844	0	//	//	//	1002	1756	1538	55,745	5145	345	28,400	158			//
Scenario IV	QOBO	//	//	//	340,787	27,085	0	18,093	921	27,759	720,800	9114	612	28,400	158			//
	BO	//	//	//	352,917	28,050	0	18,092	912	27,757	717,633	4263	286	28,400	158			//
	HHO	//	//	//	351,094	27,905	0	18,641	915	28,599	740,365	7323	491	28,400	158			//
	AEFA	//	//	//	376,885	29,955	0	18,240	887	27,985	714,885	7265	488	28,400	158			//
	IWO	//	//	//	539,845	42,907	0	20,699	774	31,757	766,838	7821	525	28,400	158			//

6.3. Sensitivity Analysis

RES is intermittent which can be affected by any variation of sizing, meteorological or economic data. The sensitivity analysis is a method that helps to select and/or to expect the optimal configuration of the hybrid system. The sensitivity analysis in this paper is implemented on the best scenario of the proposed, i.e., the PV/Biomass in the Aswan region. The selection of the sensitivity variables is based on the sizing of components in order to analyze the effect of sizing variation on four factors which are NPC, LCOE, LPSP and the Availability index.

Figure 11 shows the effect of variation in the sizing of PV and biomass units on the NPC. The PV sizing is highly impacted by the total cost of the hybrid PV/Biomass system, which means that in the case of reducing the area of PV units the NPC is reduced too. On the other hand, if the area covered by PV modules is increased, the NPC increases too. The variation in the sizing of biomass unit is increased throughout the interval -20 to 20 slowly and it has no noticeable impact on the NPC anyway. Figure 12 shows the effect of variation of PV and biomass sizing on the LCOE. The NPC and the LCOE are linked with a linear equation which means that they have the same shape. The LCOE reached 0.08 \$/kWh when the area of the PV system is reduced by 20% . Figure 13 shows the impact of variation in the sizing of PV and biomass systems on the LPSP. The impact of PV size is very important for the LPSP, because when the size of the PV system is increased the LPSP is enhanced, mainly in the -20% to 0% interval. When the PV size is changed in the interval of 0% to $+20\%$, the LPSP is increased to 2% while when the PV size is changed to -20% , the change in LPSP equals 16.4% which is a very bad sign for system building. The Biomass system does not affect the value of the LPSP and the transition between -4% to 0% is explained as the obtained sizing of the system is optimum. Figure 14 shows the impact of the variation of PV and Biomass sizing on the availability index. The availability index enhanced exponentially with the increase in the PV sizing. In the interval between -20% and 0 , availability progresses quickly, while after zero, the availability begins to be stabilized and it is clearly shown in the interval between $+12\%$ and $+20\%$.

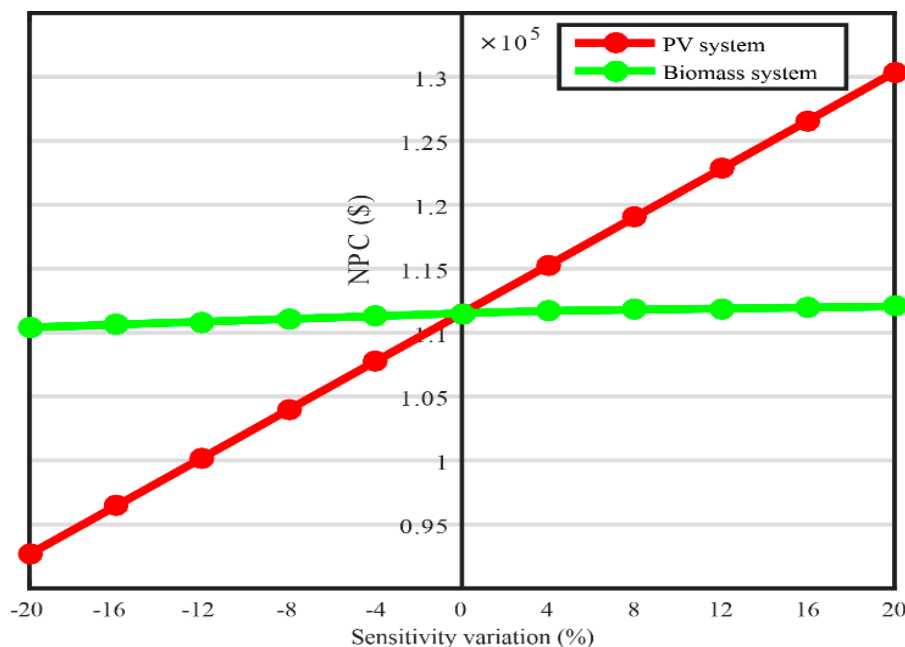


Figure 11. Sensitivity analysis application for net present cost (NPC).

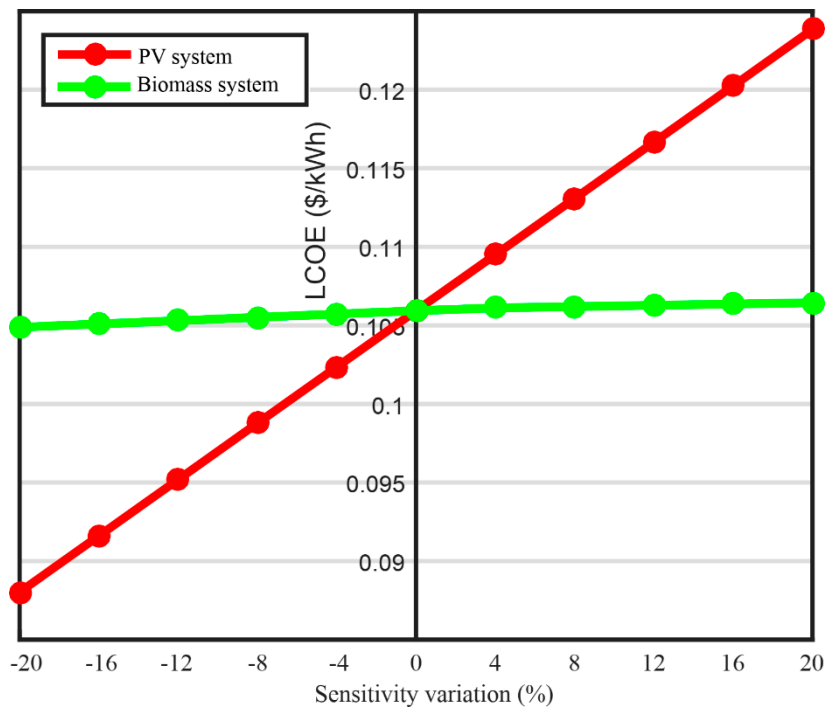


Figure 12. Sensitivity analysis application for Levelized Cost of Energy (LCOE).

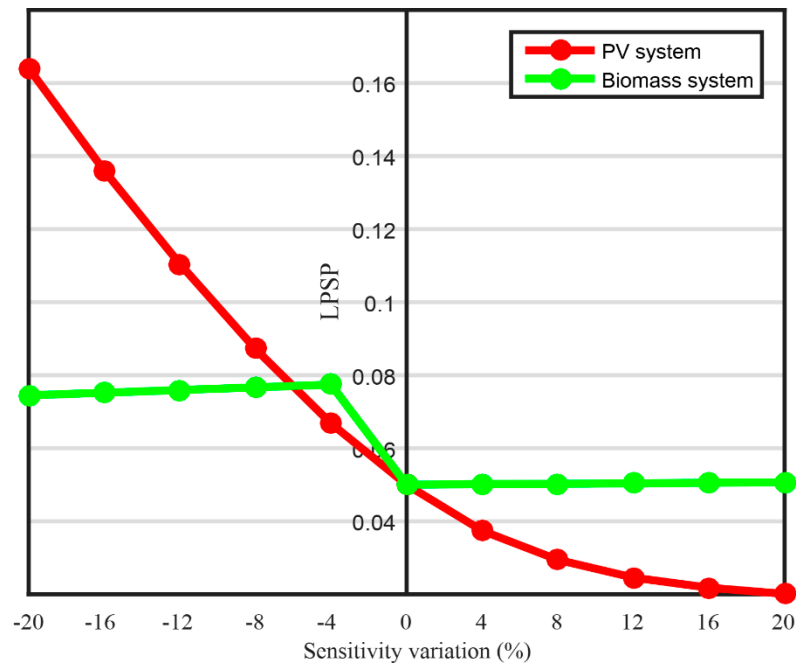


Figure 13. Sensitivity analysis application for Loss of Power Supply Probability (LPSP).

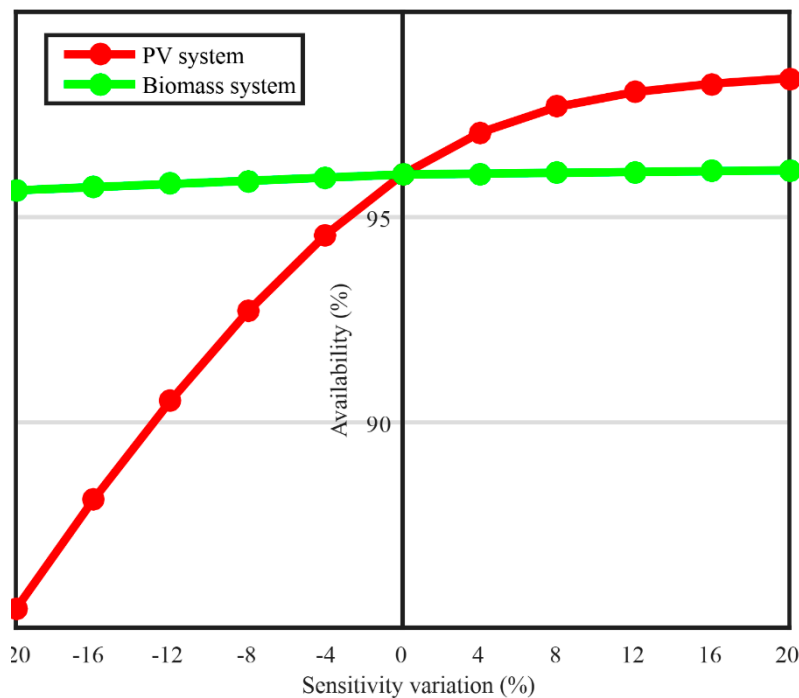


Figure 14. Sensitivity analysis application for the Availability index.

The PV system through this analysis is demonstrated as a very important element for having a high hybrid systems criterion. However, the Biomass system helps the PV to satisfy the constraints and its variation does not have a serious impact on the performance of the hybrid system.

7. Conclusions

With the increased penetration level of RES into electrical energy production in the microgrid systems, new challenges have emerged on the international scene. These challenges are represented in finding ways to optimize the design of the hybrid system by using smart algorithms and software. Among these dilemmas, the economic cost and feasibility of installing systems in different locations in the world is considered the most important challenge. Therefore, this research proposes a developed algorithm called Quasi-Oppositional Bonobo Optimizer (QOBO) for the optimal economic design of a stand-alone hybrid microgrid system in Aswan, Egypt. Four configurations of the hybrid system have been implemented, which consist of RES (PV panels, WT and biomass) with diesel generators and battery storage systems. The obtained results showed that the PV/Biomass scenario is the most cost-effective system with an NPC of \$110,807 and LCOE of 0.1053 \$/kWh; otherwise, the best configuration of the microgrid system contained 293.971 m² of PV and 1020.18 ton/year consumed by the biomass system; the PV/Diesel/BESS scenario is also cost-effective with NPC of \$153,401 and LCOE of 0.1457 \$/kWh. On the other side, the LPSP and availability index are satisfied and without the need for traditional resources. Additionally, the results showed the ability of the QOBO algorithm to reach the optimal solution in a shorter time and with better efficiency compared to the traditional BO, HHO, AEFA and IWO algorithms in all cases studies. Furthermore, a sensitivity analysis of the proposed systems scenarios was performed to obtain the impact of unit size on the performance of the hybrid system, where it has been emphasized that PV system sizing is very important and has a great impact on the overall performance of the system. The obtained results from this study would be useful material for decision makers working on the development of the renewable energy sector in Egypt. In future studies, it is suggested to apply the proposed QOBO in other engineering problems.

Author Contributions: Conceptualization, S.K. and M.K.; Data curation, O.H.M., H.M.S. and A.S.; Formal analysis, F.J., M.A. and H.M.S.; Methodology, M.K., A.S. and S.K.; Resources, O.H.M., S.K. and H.M.S.; Software,

A.S., M.K.; Supervision, F.J.; Validation, H.M.S. and O.H.M.; Visualization, S.K., A.S. and M.A.; Writing—original draft, M.K., O.H.M., A.S. and H.M.S.; Writing—review & editing, S.K., M.A. and F.J. All authors together organized and refined the manuscript in the present form. All authors have approved the final version of the submitted paper. All authors have read and agreed to the published version of the manuscript.

Funding: This work was supported in part by the NSFC, China-ASRT, Egypt, Joint Research Fund, under Grant 51861145406.

Acknowledgments: The authors gratefully acknowledge the contribution of the NSFC (China)-ASRT (Egypt) Joint Research Fund, Project No. 51861145406 for providing partial research funding to the work reported in this research.

Conflicts of Interest: The authors declare no conflict of interest.

Nomenclature

Symbols

A	Availability index	η_b	Efficiency of the battery (%)
A_g	Coefficient of consumption curve ($a = 0.246$ L/kW)	η_{bio}	Efficiency of the biomass system (%)
AD	Daily autonomy of the battery (day)	η_{inv}	Efficiency of the inverter (%)
A_{pv}	Area covered by PV panels (m^2)	η_{pv}	Efficiency of the PV system (%)
A_{tt}	Cross-sectional area of the tidal (m^2)	η_r	Reference efficiency of PV panels (%)
A_{wind}	Swept area by the wind turbine (m^2)		
C	Capital Cost (\$)	P_{wind}	Output power of the wind turbine (kW)
$C_{Battery}$	Capacity of the Battery (kWh)	R	Replacement Cost (\$)
C_p	Maximum power coefficient (%)	T	Temperature ($^{\circ}C$)
CV_{bio}	Calorific value of the organic material (MJ/kg)	T_a	Ambient temperature ($^{\circ}C$)
DOD	Depth of Discharge (%)	$Total_{av}$	Total biomass available (t/yr)
E_l	Load demand (kWh)	T_r	Reference temperature of solar cell ($^{\circ}C$)
F_{dg}	Fuel consumption of the diesel generator (L/h)	V	Wind speed (m/s)
FC_{dg}	Fuel Cost for one year (\$/Year)	V_{ci}	Cut-in wind speed (m/s)
I	Solar irradiation (kW/ m^2)	V_{co}	Cut-out wind speed (m/s)
i_r	Interest rate (%)	V_r	Rated wind speed (m/s)
N	project lifetime (year)	B_g	Coefficient of consumption curve ($b = 0.08415$ L/kW)
$NOCT$	Nominal operating cell temperature ($^{\circ}C$)	η_t	Efficiency MPPT system (%)
NPC	Net Present Cost (\$)	β	Temperature coefficient (0.004 to 0.006 $^{\circ}C$)
OM	Maintenance and Operation (\$)	ρ	Air density (Kg/ m^3)
P_{dg}	Rated power of the diesel generator (kW)	λ_{bat}	Initial cost of the battery system (\$/kWh)
P_f	Fuel price (\$/L)	λ_{bg}	Initial cost of biomass system (\$/kW)
P_{bg}	Generated power of the biogas plant (kW)	λ_{dg}	Initial cost of diesel generator (\$/kW)
P_{BM}	Biomass power (kW)	$\lambda_{PV,WT}$	Initial cost of PV and WT (\$/ m^2)
P_{pv}	Output power of the PV (kW)	δ	Inflation rate (%)
P_r	Rated power (kW)	μ	Escalation rate (%)
P_{re}	Power from renewable energy systems	θ_1	Biomass annual fixed O&M cost (\$/kW/year)
P_w	Annual working of biomass (kWh/Year)	θ_2	Biomass variable O&M cost (\$/kW h)

Acronyms

AEFA	Artificial Electric Field Algorithm	HSA	Harmony Search Algorithm
ACS	Annualized cost of the system	IWO	Invasive Weed optimization Algorithm
BESS	Battery Energy Storage System	LCOE	Levelized Cost of Energy
BO	Bonobo Optimizer Algorithm	LPSP	Loss of Power Supply Probability
BOQO	Improved Quasi Oppositional BO Algorithm	MOPSO	Multiple Objective Particle Swarm Optimization
COE	Cost of Energy	NPC	Net present cost
CRF	Capital Recovery Factor	PSO	Particle Swarm Optimization
HOMER	Hybrid Optimization of Multiple Energy Resources	PV	Photovoltaic
HRES	Hybrid Renewable Energy Systems	RF	Renewable Fraction
HHO	Harris Hawks Optimization	WT	Wind Turbine

Appendix A. Algorithms

Appendix A.1. Harris Hawks Optimization Algorithm

Heidari and et al. [36] proposed a new nature-inspired optimization algorithm called Harris Hawks Optimizer. They were inspired by the cooperative behavior and chasing style of Harris hawks. The modeling of this technique is based firstly on an exploration phase; afterwards, the transition from exploration to exploitation, then the

exploitation phase and, finally, the soft besiege. The modeling is taken on for all strategies for exploring a prey, surprise pounce and different attacking methods of Harris hawks. The pseudo-code of the HHO algorithm is proposed below.

Algorithm A1: Pseudo code of HHO

Initialize the population size and max iteration (K_{max})
 Initialize a set random rabbit location, within the limits $X_{min}^i \leq X_{rabbit}^i \leq X_{max}^i$.
 Evaluate the objective function for all rabbits
 While ($k < K_{max}$)
 Calculate the fitness of hawks
 Set x_{rabbit} in the best location
 for each hawk do
 Update the initial energy E_0 , energy E and jump strength J ;
 $E_0 = 2rand() - 1$, $E = 2E_0(1 - \frac{k}{T})$, $J = 2(1 - rand())$
 if ($|E| \geq 1$) then
 Exploration phase
 if ($|E| < 1$) then
 Exploitation phase
 if ($r \geq 0.5$ and $|E| \geq 0.5$) then
 Soft besiege
 else if ($r \geq 0.5$ and $|E| < 0.5$) then
 Hard besiege
 else if ($r < 0.5$ and $|E| \geq 0.5$) then
 Soft besiege with progressive rapid dives
 else if ($r < 0.5$ and $|E| < 0.5$) then
 Hard besiege with progressive rapid dives
 Return x_{rabbit}

Appendix A.2. Artificial Electric Field Algorithm

Anita and Yadav [37] were inspired by Coulomb's law of electrostatic force to create a novel artificial electric field algorithm. The concepts of electric field and charged particles provide us a strong theory for the working force of attraction or repulsion between two charged particles. The pseudo code of the AEFA algorithm is proposed in Algorithm A2.

Algorithm A2: Pseudo code of AEFA

Initialize a set of random population $X_B^i = (X_B^1, X_B^2, \dots, X_B^N)$ of N size, within the limits $X_{min}^i \leq X_B^i \leq X_{max}^i$.
 Initialize the velocity to a random value
 Evaluate the fitness of whole population
 Set the iteration to zero
 Reproduction and Updating
 While criteria not satisfied do
 Calculate $K(t)$, best (t) and worst (t)
 for $i = 1: N$ do
 Evaluate the fitness values
 Calculate the total force in each direction
 Calculate the acceleration
 $V_i(t+1) = rand() \times V_i(t) + a_i(t)$
 $X_i(t+1) = X_i(t) + V_i(t+1)$
 end for
 end while

Appendix A.2.1. Invasive Weed Optimization Algorithm

Invasive weed optimization is a numerical stochastic optimization algorithm inspired by colonizing weeds, which was introduced in 2006 by Mehrabian and Lucas [38]. In IWO, a certain number of weeds make up the

whole population, and each weed comprises a set of decision variables. Weeds are a serious threat to desirable plants because they are plants that are invasive and hardy.

Weeds are plants which are vigorous and invasive; they pose a serious threat to desirable, cultivated plants in agriculture. Weeds have shown to be very robust and adaptive to change in the environment. The IWO optimization algorithm has been modeled based on four steps: initialization, reproduction, spatial dispersal and competitive exclusion.

- *Initialization and Production*

Firstly, the population is spread over the research space randomly; afterwards, each plant is allowed to produce seeds depending on its own fitness; the production of seeds is not only allowed for the better plants' fitness as in the other evolutionary algorithms, but the reproduction step of IWO is also proposed to give a chance to infeasible individuals to survive and reproduce similar to the mechanism which occurs in nature. The weeds producing seeds can be formulated as follows:

$$Weed_n = \frac{f - f_{min}}{f_{max} - f_{min}} (s_{max} - s_{min}) + s_{min} \quad (A1)$$

where in each iteration, f is the current weed's fitness. f_{max} and f_{min} represent the max and min fitness values, respectively. s_{max} and s_{min} represent the max and min values of the weeds, respectively.

- *Spatial Dispersal*

The generated seeds are being randomly distributed over the search space such that they abode near the parent plant. However, the standard deviation (σ) of the random function will be reduced in every iteration, the nonlinear alteration equation of the standard deviation at each iteration is presented as follows:

$$\sigma_{inter} = \frac{(iter_{max} - iter)^n}{(iter_{max})^n} (\sigma_{initial} - \sigma_{final}) + \sigma_{final} \quad (A2)$$

where $iter_{max}$ is the maximum iteration, n is the nonlinear modulation index, $\sigma_{initial}$ and σ_{final} are the initial and final values of standard deviation, respectively.

- *Competitive Exclusion*

In a colony, the maximum number allowed of plants is limited; for that, competitive exclusion is applied. The plant that leave no offspring would go extinct; otherwise, they can survive. After some iterations, the number of plants in a colony will reach its maximum through the reproduction step, the seeds and their parents are ranked together, and all plants in the research space are considered as weeds; afterwards, weeds with lower fitness are eliminated.

The overall steps of the IWO algorithm are presented in Algorithm A3.

Algorithm A3: Pseudo code of IWO

Initialize a set of random weeds, $weed_B^i = (weed_B^1, weed_B^2, \dots, weed_B^N)$ within the limits $weed_{min}^i \leq weed_B^i \leq weed_{max}^i$.
 Set the IWO's parameters
 Evaluate the objective function for all weeds
 While ($iter < iter_{max}$)
 Calculate the best and worst fitness in the colony
 Calculate the σ
 for each weed in the colony
 Calculate the number of seeds following the fitness of each weed
 Add the seeds to their parents in the colony
 if $Size_{max} \leq Nb_{population}$
 Sort the new population according to their fitness
 Eliminate the worst fitness in order to achieve the $Size_{max}$ allowed
 end if
 end for
 Update iteration $iter = iter + 1$
 end while
 Return the final best solution

References

1. Kharrich, M.; Mohammed, O.H.; Mohammed, Y.S.; Akherraz, M. A Review on Recent Sizing Methodologies for Hybrid Microgrid Systems. *Int. J. Energy Convers.* **2019**, *7*, 230–240. [[CrossRef](#)]
2. Babatunde, O.M.; Munda, J.L.; Hamam, Y. A Comprehensive State-of-the-Art Survey on Hybrid Renewable Energy System Operations and Planning. *IEEE Access* **2020**, *8*, 75313–75346. [[CrossRef](#)]
3. Khatib, H. IEA world energy outlook 2011—A comment. *Energy Policy* **2012**, *48*, 737–743. [[CrossRef](#)]
4. Zhang, W.; Maleki, A.; Rosen, M.A.; Liu, J. Optimization with a simulated annealing algorithm of a hybrid system for renewable energy including battery and hydrogen storage. *Energy* **2018**, *163*, 191–207. [[CrossRef](#)]
5. Diab, A.A.Z.; Sultan, H.M.; Mohamed, I.S.; Kuznetsov, O.N.; Do, T.D. Application of different optimization algorithms for optimal sizing of PV/wind/diesel/battery storage stand-alone hybrid microgrid. *IEEE Access* **2019**, *7*, 119223–119245. [[CrossRef](#)]
6. Diab, A.A.Z.; Sultan, H.M.; Kuznetsov, O.N. Optimal sizing of hybrid solar/wind/hydroelectric pumped storage energy system in Egypt based on different meta-heuristic techniques. *Environ. Sci. Pollut. Res.* **2019**, *27*, 1–23. [[CrossRef](#)]
7. Mohammed, O.; Amirat, Y.; Benbouzid, M.; Feld, G. Optimal Design and Energy Management of a Hybrid Power Generation System Based on Wind/Tidal/Pv Sources: Case Study for the Ouessant French Island. In *Smart Energy Grid Design for Island Countries*; Springer: Berlin/Heidelberg, Germany, 2017; pp. 381–413.
8. Lian, J.; Zhang, Y.; Ma, C.; Yang, Y.; Chaima, E. A review on recent sizing methodologies of hybrid renewable energy systems. *Energy Convers. Manag.* **2019**, *199*, 112027. [[CrossRef](#)]
9. Yadav, D.K.; Girimaji, S.P.; Bhatti, T.S. Optimal Hybrid Power System Design Using HOMER. In Proceedings of the 2012 IEEE 5th India International Conference on Power Electronics (IICPE), Delhi, India, 6–8 December 2012; pp. 1–6.
10. Mohammed, O.H. Optimal Hybridisation of a Renewable System to Fulfill Residential Electrical Load: In Mosul, Iraq. In Proceedings of the 2018 Third Scientific Conference of Electrical Engineering (SCEE), Baghdad, Iraq, 9–20 December 2018; IEEE: Piscataway, NJ, USA, 2018; pp. 209–213.
11. Papaefthymiou, S.V.; Papathanassiou, S.A. Optimum sizing of wind-pumped-storage hybrid power stations in island systems. *Renew. Energy* **2014**, *64*, 187–196. [[CrossRef](#)]
12. Hazem Mohammed, O.; Amirat, Y.; Benbouzid, M. Economical evaluation and optimal energy management of a stand-alone hybrid energy system handling in genetic algorithm strategies. *Electronics* **2018**, *7*, 233. [[CrossRef](#)]
13. Rezk, H.; Al-Dhaifallah, M.; Hassan, Y.B.; Ziedan, H.A. Optimization and Energy Management of Hybrid Photovoltaic-Diesel-Battery System to Pump and Desalinate Water at Isolated Regions. *IEEE Access* **2020**, *8*, 102512–102529. [[CrossRef](#)]
14. Wang, R.; Xiong, J.; He, M.-F.; Gao, L.; Wang, L. Multi-objective optimal design of hybrid renewable energy system under multiple scenarios. *Renew. Energy* **2020**, *151*, 226–237. [[CrossRef](#)]
15. Nandi, S.K.; Ghosh, H.R. Prospect of wind-PV-battery hybrid power system as an alternative to grid extension in Bangladesh. *Energy* **2010**, *35*, 3040–3047. [[CrossRef](#)]
16. Khan, M.; Iqbal, M. Pre-feasibility study of stand-alone hybrid energy systems for applications in Newfoundland. *Renew. Energy* **2005**, *30*, 835–854. [[CrossRef](#)]
17. Sen, R.; Bhattacharyya, S.C. Off-grid electricity generation with renewable energy technologies in India: An application of HOMER. *Renew. Energy* **2014**, *62*, 388–398. [[CrossRef](#)]
18. Hemeida, A.; El-Ahmar, M.; El-Sayed, A.; Hasanien, H.M.; Alkhalaf, S.; Esmail, M.; Senjyu, T. Optimum design of hybrid wind/PV energy system for remote area. *Ain Shams Eng. J.* **2020**, *11*, 11–23. [[CrossRef](#)]
19. Xu, X.; Hu, W.; Cao, D.; Huang, Q.; Chen, C.; Chen, Z. Optimized sizing of a standalone PV-wind-hydropower station with pumped-storage installation hybrid energy system. *Renew. Energy* **2020**, *147*, 1418–1431. [[CrossRef](#)]
20. Barbaro, M.; Castro, R. Design optimisation for a hybrid renewable microgrid: Application to the case of Faial island, Azores archipelago. *Renew. Energy* **2020**, *151*, 434–445. [[CrossRef](#)]
21. Alshammari, N.; Asumadu, J. Optimum Unit Sizing of Hybrid Renewable Energy System Utilizing Harmony Search, Jaya and Particle Swarm Optimization Algorithms. *Sustain. Cities Soc.* **2020**, *60*, 102255. [[CrossRef](#)]

22. Das, A.K.; Pratihari, D.K. A New Bonobo Optimizer (BO) for Real-Parameter Optimization. In Proceedings of the 2019 IEEE Region 10 Symposium (TENSYPMP), Kolkata, India, 7–9 June 2019; IEEE: Piscataway, NJ, USA, 2019; pp. 108–113.
23. Kharrich, M.; Mohammed, O.H.; Akherraz, M. Assessment of Renewable Energy Sources in Morocco using Economical Feasibility Technique. *Int. J. Renew. Energy Res.* **2019**, *9*, 1856–1864.
24. Kharrich, M.; Mohammed, O.H.; Akherraz, M. Design of Hybrid Microgrid PV/Wind/Diesel/Battery System: Case Study for Rabat and Baghdad. *EAI Endorsed Trans. Energy Web* **2020**, *7*. [[CrossRef](#)]
25. Ramli, M.A.M.; Bouchekara, H.R.E.H.; Alghamdi, A.S. Optimal sizing of PV/wind/diesel hybrid microgrid system using multi-objective self-adaptive differential evolution algorithm. *Renew. Energy* **2018**, *121*, 400–411. [[CrossRef](#)]
26. Ghiasi, M. Detailed study, multi-objective optimization, and design of an AC-DC smart microgrid with hybrid renewable energy resources. *Energy* **2019**, *169*, 496–507. [[CrossRef](#)]
27. Movahediyani, Z.; Askarzadeh, A. Multi-objective optimization framework of a photovoltaic-diesel generator hybrid energy system considering operating reserve. *Sustain. Cities Soc.* **2018**, *41*, 1–12. [[CrossRef](#)]
28. Heydari, A.; Askarzadeh, A. Optimization of a biomass-based photovoltaic power plant for an off-grid application subject to loss of power supply probability concept. *Appl. Energy* **2016**, *165*, 601–611. [[CrossRef](#)]
29. Sultan, H.M.; Menesy, A.S.; Kamel, S.; Tostado-Véliz, M.; Jurado, F. Parameter Identification of Proton Exchange Membrane Fuel Cell Stacks Using Bonobo Optimizer. In Proceedings of the 2020 IEEE International Conference on Environment and Electrical Engineering and 2020 IEEE Industrial and Commercial Power Systems Europe (EEEIC/I&CPS Europe), Madrid, Spain, 9–12 June 2020; IEEE: Piscataway, NJ, USA, 2020; pp. 1–7.
30. Tizhoosh, H.R. Opposition-Based Learning: A New Scheme for Machine Intelligence. In Proceedings of the International Conference on Computational Intelligence for Modelling, Control and Automation and International Conference on Intelligent Agents, Web Technologies and Internet Commerce (CIMCA-IAWTIC'06), Vienna, Austria, 28–30 November 2005; IEEE: Piscataway, NJ, USA, 2005; pp. 6957–6961.
31. Roy, P.K.; Bhui, S. Multi-objective quasi-oppositional teaching learning based optimization for economic emission load dispatch problem. *Int. J. Electr. Power Energy Syst.* **2013**, *53*, 937–948. [[CrossRef](#)]
32. Sultana, S.; Roy, P.K. Multi-objective quasi-oppositional teaching learning based optimization for optimal location of distributed generator in radial distribution systems. *Int. J. Electr. Power Energy Syst.* **2014**, *63*, 534–545. [[CrossRef](#)]
33. Sharma, S.; Bhattacharjee, S.; Bhattacharya, A. Quasi-Oppositional Swine Influenza Model Based Optimization with Quarantine for optimal allocation of DG in radial distribution network. *Int. J. Electr. Power Energy Syst.* **2016**, *74*, 348–373. [[CrossRef](#)]
34. Yu, J.; Kim, C.-H.; Rhee, S.-B. Oppositional Jaya Algorithm With Distance-Adaptive Coefficient in Solving Directional Over Current Relays Coordination Problem. *IEEE Access* **2019**, *7*, 150729–150742. [[CrossRef](#)]
35. Abd Elaziz, M.; Mirjalili, S. A hyper-heuristic for improving the initial population of whale optimization algorithm. *Knowl. Based Syst.* **2019**, *172*, 42–63. [[CrossRef](#)]
36. Heidari, A.A.; Mirjalili, S.; Faris, H.; Aljarah, I.; Mafarja, M.; Chen, H. Harris hawks optimization: Algorithm and applications. *Future Gener. Comput. Syst.* **2019**, *97*, 849–872. [[CrossRef](#)]
37. Yadav, A. AEFA: Artificial electric field algorithm for global optimization. *Swarm Evol. Comput.* **2019**, *48*, 93–108.
38. Mehrabian, A.R.; Lucas, C. A novel numerical optimization algorithm inspired from weed colonization. *Ecol. Inform.* **2006**, *1*, 355–366. [[CrossRef](#)]

